Generalizing Camera Models

CS535

Daniel G. Aliaga
Department of Computer Science
Purdue University

Multiperspective Imaging

Hand-crafted

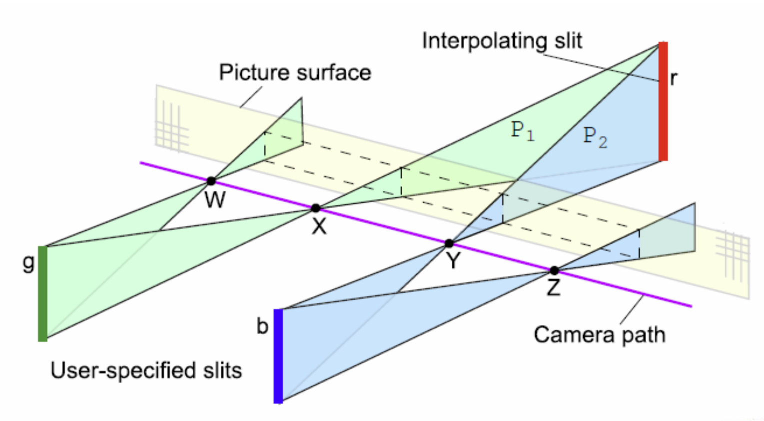

semi-automated…

to produce this…

[Roman-Vis04]

Multiperspective Imaging

[Seitz-CGA03]

Multiple COP Images

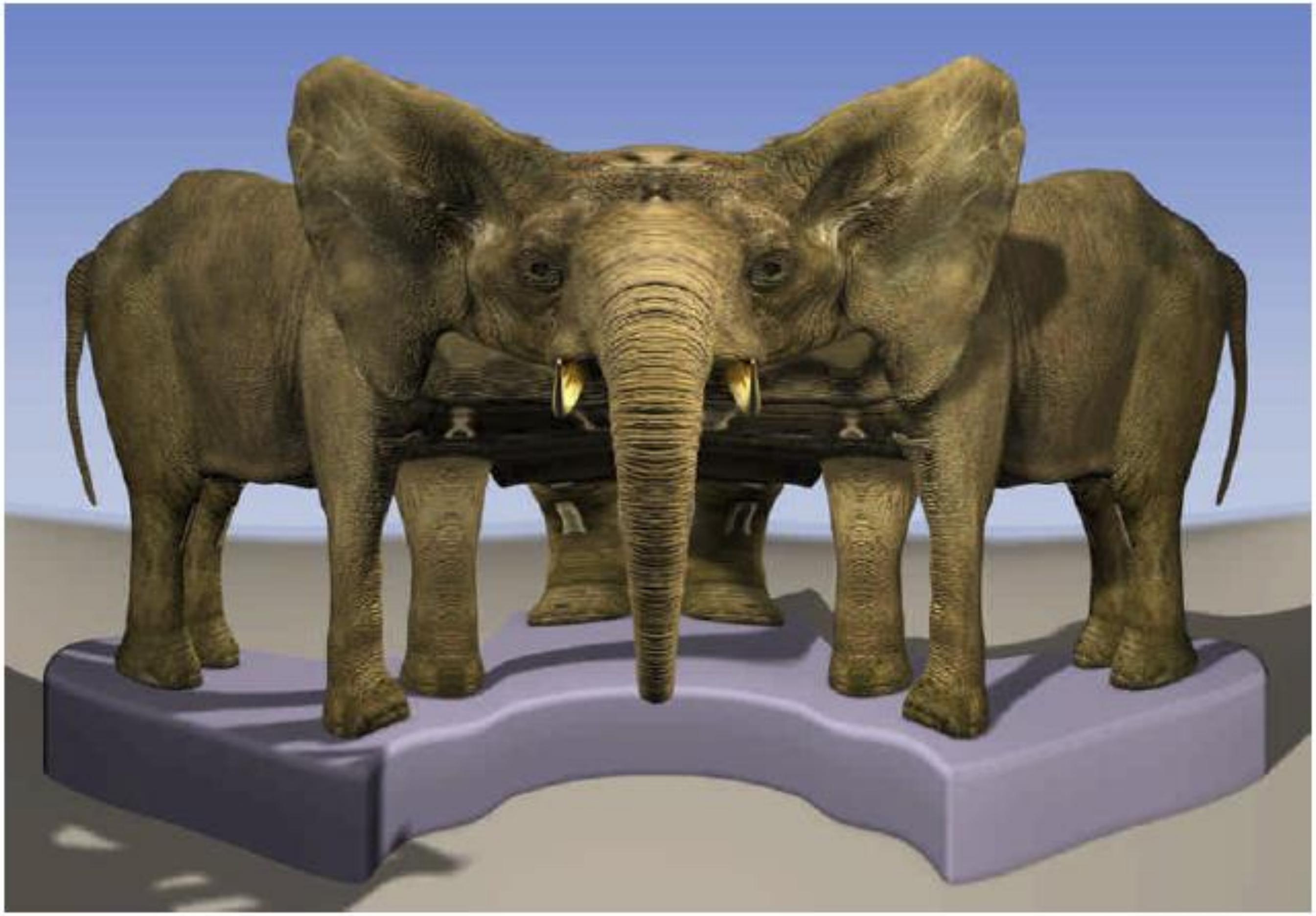

[Rademacher-SIG98]

Multiple COP Images

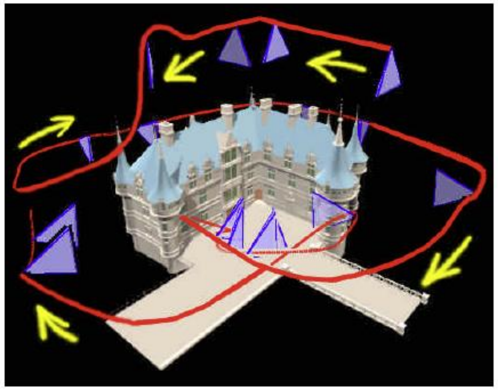

Figure 5 Castle model. The red curve is the path the camera was swept on, and the arrows indicate the direction of motion. The blue triangles are the thin frusta of each camera. Every 64th camera is shown.

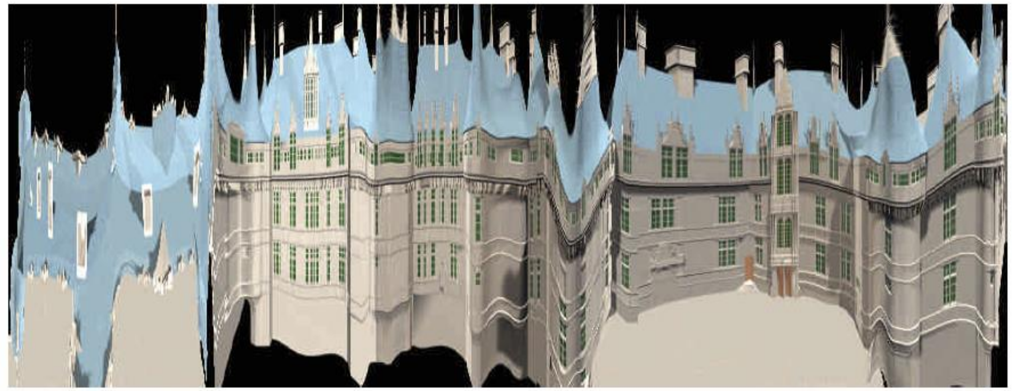

Figure 6 The resulting 1000×500 MCOP image. The first fourth of the image, on the left side, is from the camera sweeping over the roof. Note how the courtyard was sampled more finely, for added resolution.

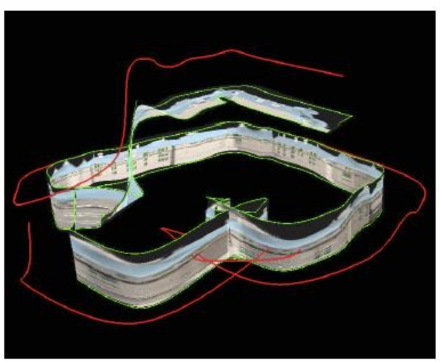

Figure 7 The projection surface (image plane) of the camera curve.

Figure 8 Three views of the castle, reconstructed solely from the single MCOP image above. This dataset captures the complete exterior of the castle.

[Rademacher-SIG98]

Multiperspective Imaging for Cel Animation

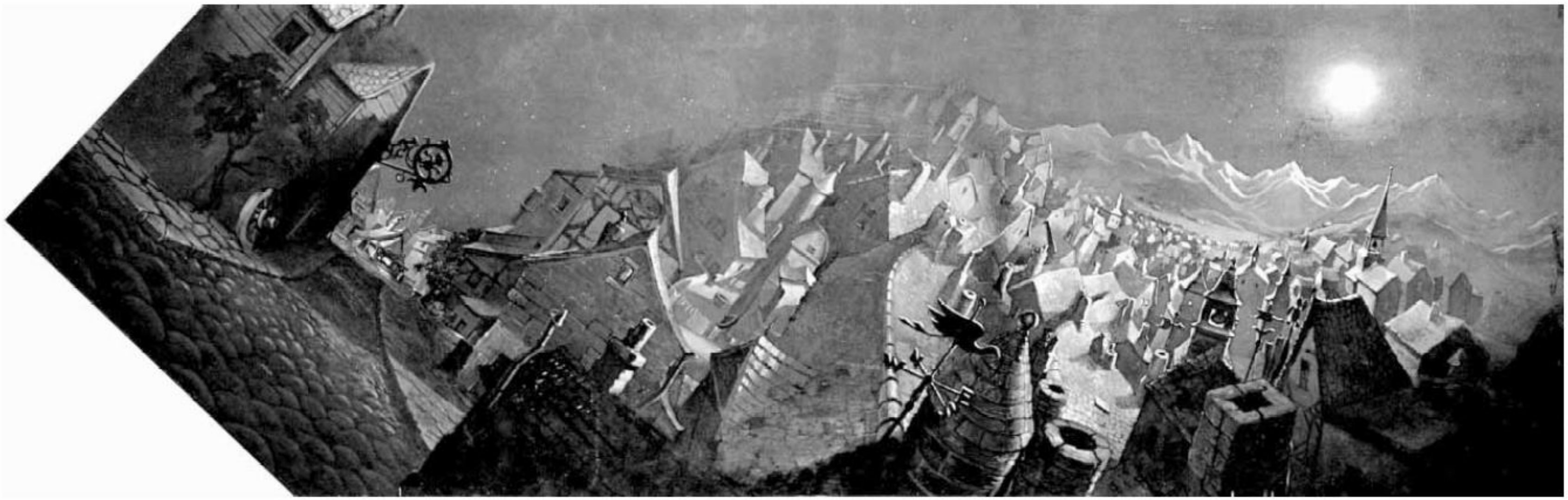

Figure 1 A multiperspective panorama from Disney's 1940 film *Pinocchio*. (Used with permission.)

Multiperspective Imaging for Cel Animation

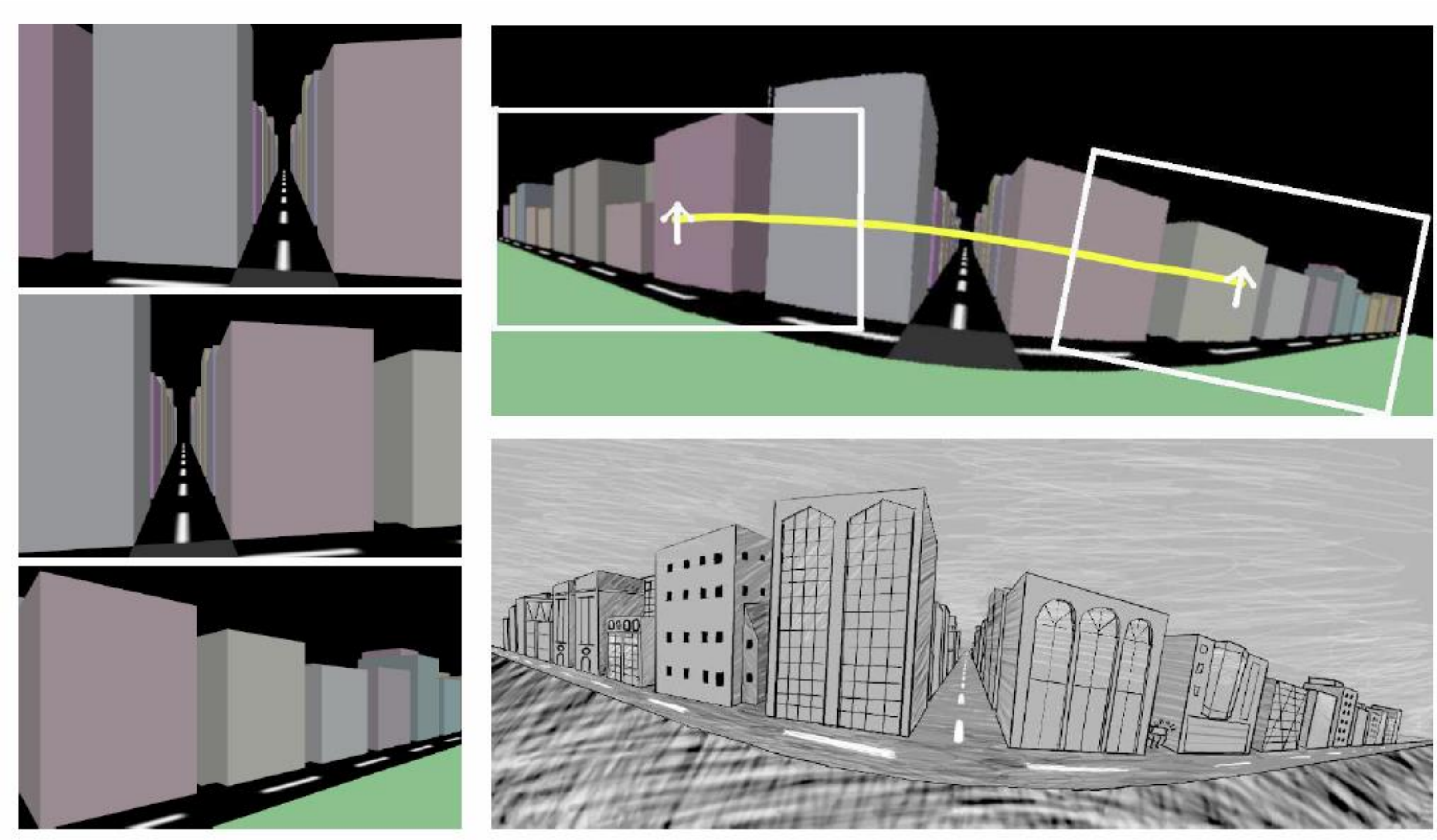

[Wood-SIG97]

Multiperspective Imaging for Cel Animation

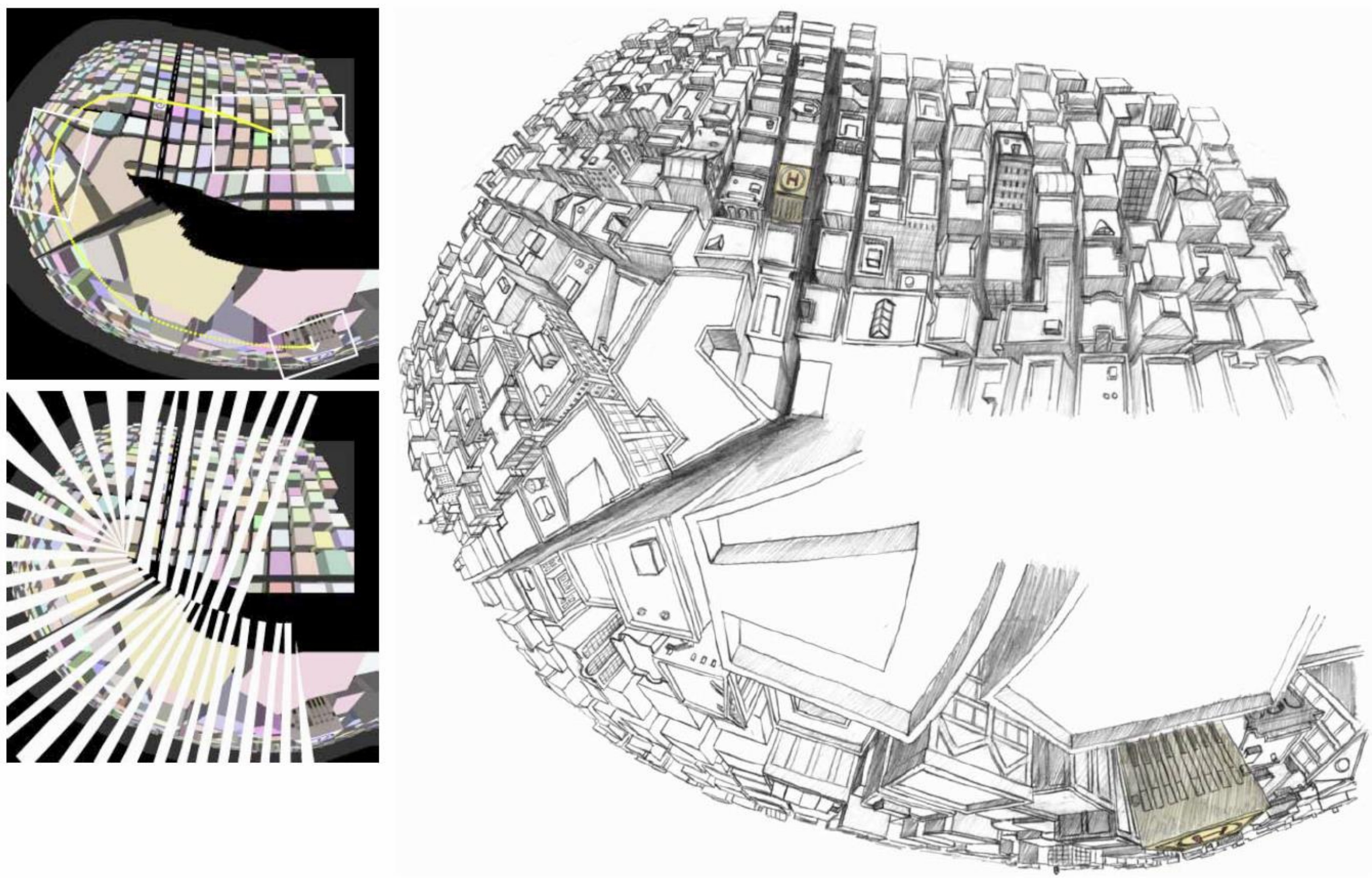

[Wood-SIG97]

Multiperspective Imaging for Cel Animation

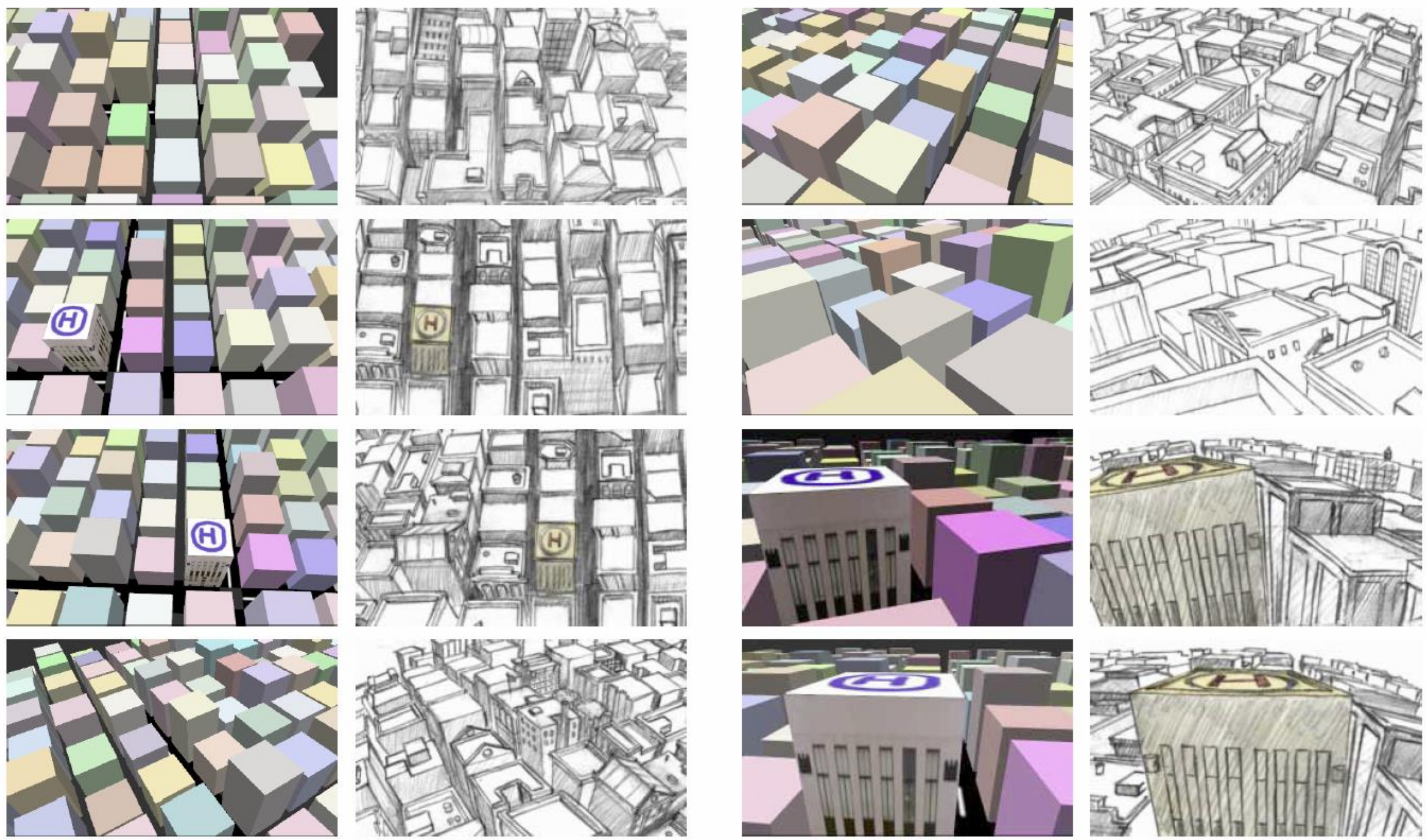

[Wood-SIG97]

Occlusion-Resistant Cameras

Input images

Output images

[Aliaga-CGA07]

Occlusion-Resistant Cameras

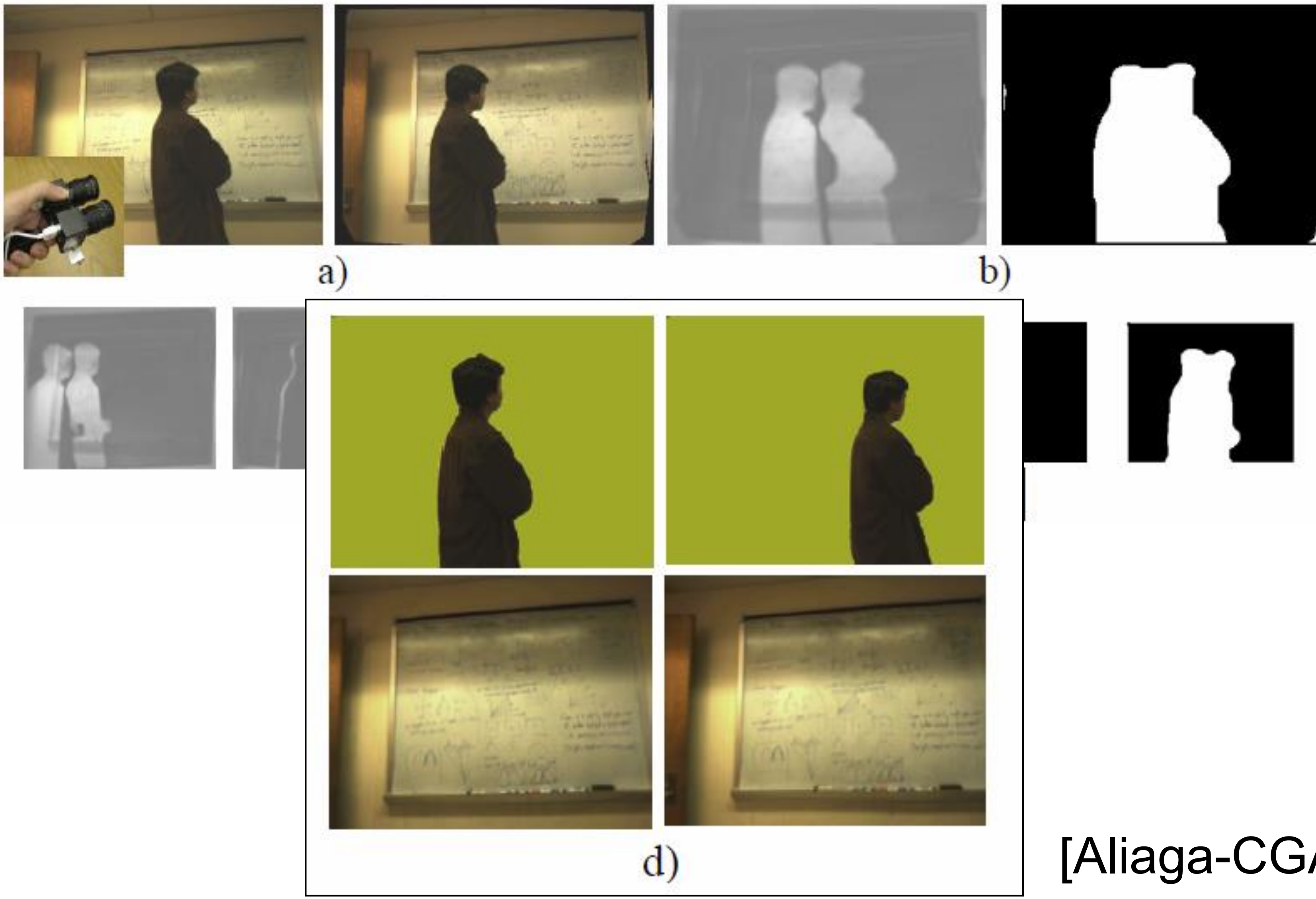

[Aliaga-CGA07]

Occlusion-Resistant Cameras

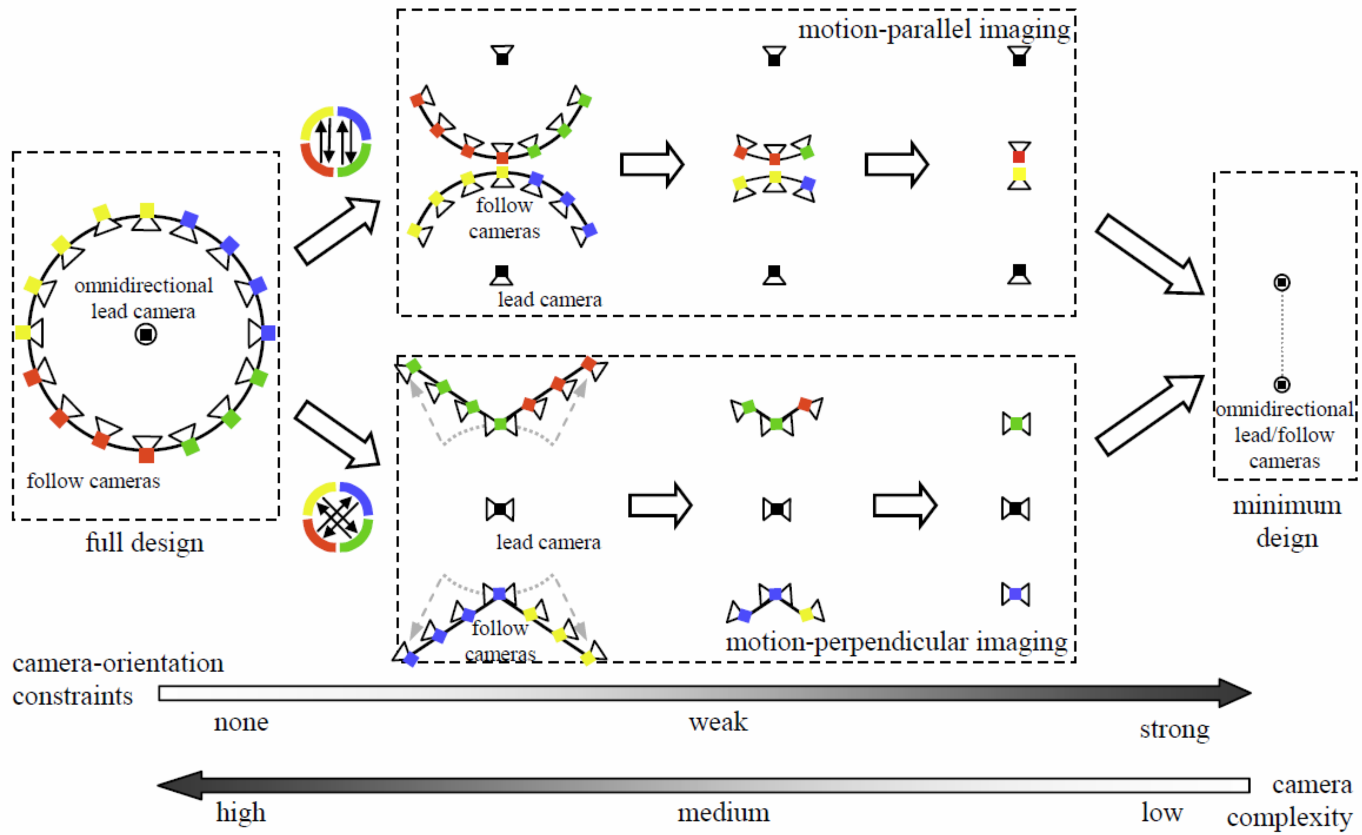

Figure 1. Family of ORC Designs. *This diagram shows 2D versions of our family of cameras. Individual cameras are represented by small (colored) squares. The camera's field-of-view is drawn using a small triangle for limited field-of-view cameras and as a circle for omnidirectional cameras. Left: a full design of a sphere of follow cameras (color-coded) surrounding an omnidirectional lead camera (black) produces occlusion-resistant images for all imaging directions and camera orientations. Middle: progressively simpler cameras require stricter control of the camera's orientation, providing*

[Aliaga-CGA07]

Occlusion Cameras

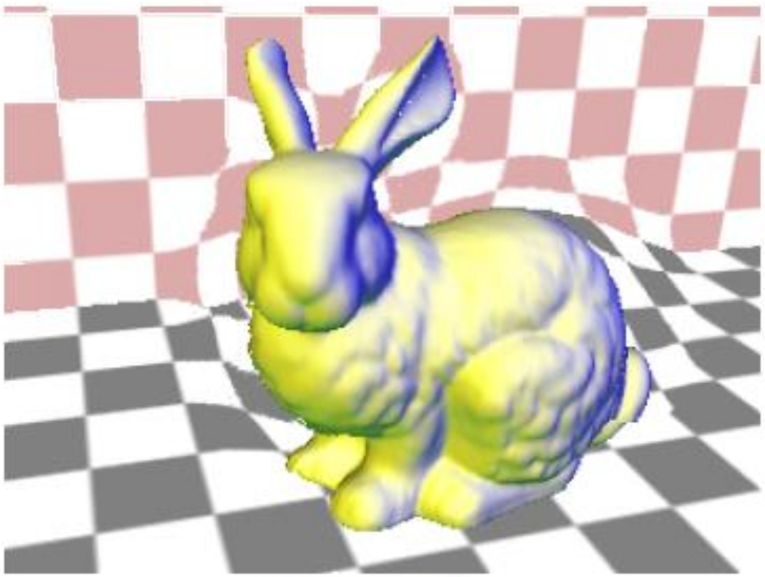

DDOC reference image.

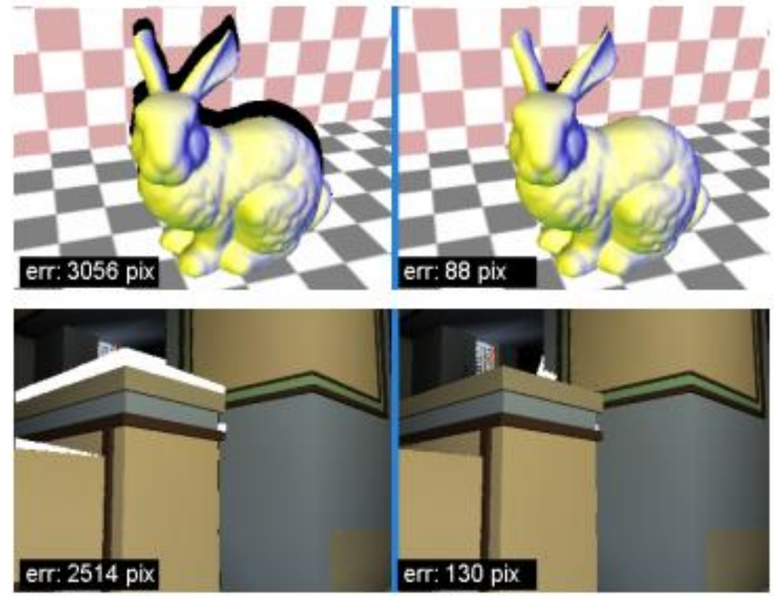

Frames rendered from depth image and DDOC image

[Popescu-I3D06]

Occlusion Cameras

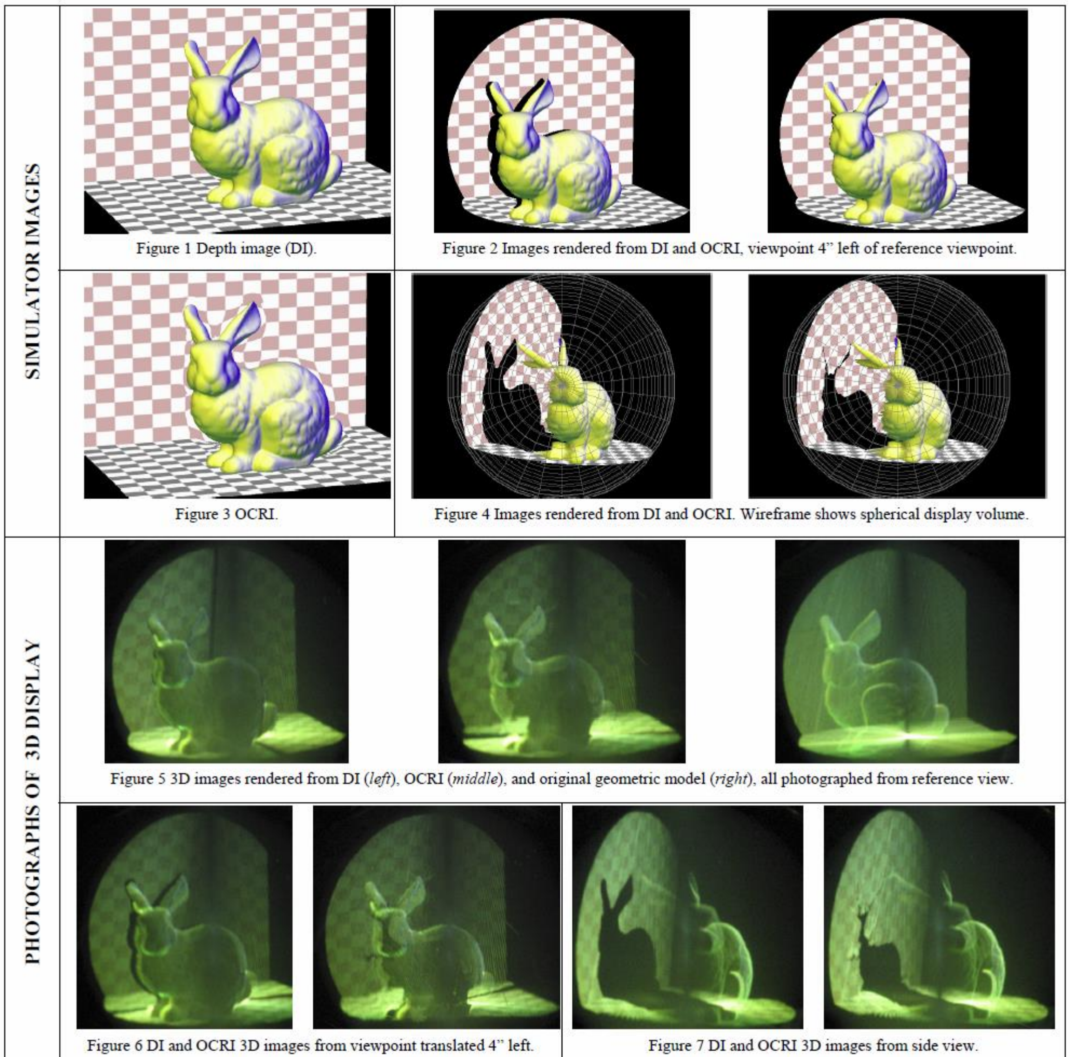

Figure 1 Depth image (DI).

Figure 2 Images rendered from DI and OCRI, viewpoint 4" left of reference viewpoint.

Figure 3 OCRI.

Figure 4 Images rendered from DI and OCRI. Wireframe shows spherical display volume.

Figure 5 3D images rendered from DI (*left*), OCRI (*middle*), and original geometric model (*right*), all photographed from reference view.

Figure 6 DI and OCRI 3D images from viewpoint translated 4" left.

Figure 7 DI and OCRI 3D images from side view.

[Popescu-JDT06]

Graph Cameras

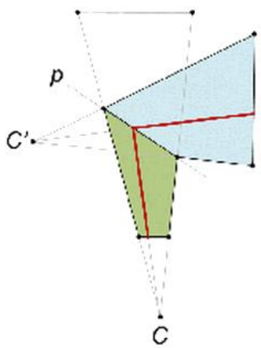

Bend Operation

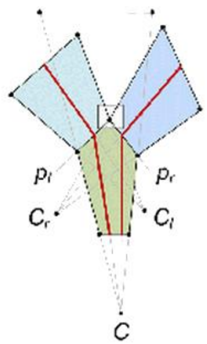

Split Operation

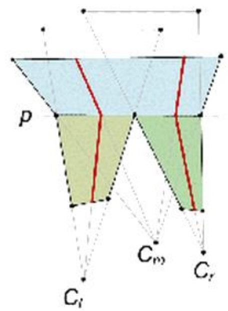

Merge Operation

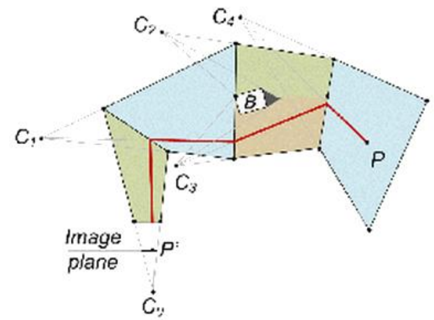

Graph Camera Frustum

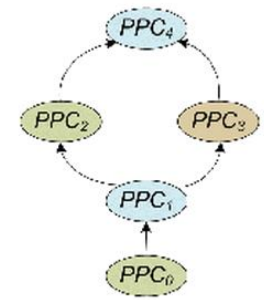

Graph of Frusta

[Popescu-SIGA09]

Graph Cameras

Portal-based graph camera image (top left and fragment right) and PPC image for comparison (bottom left)

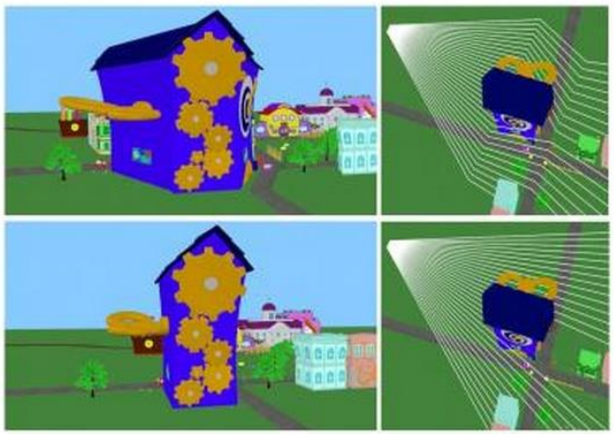

Occluder-based graph camera image (top left), PPC image for comparison (bottom left), and ray visualizations (right)

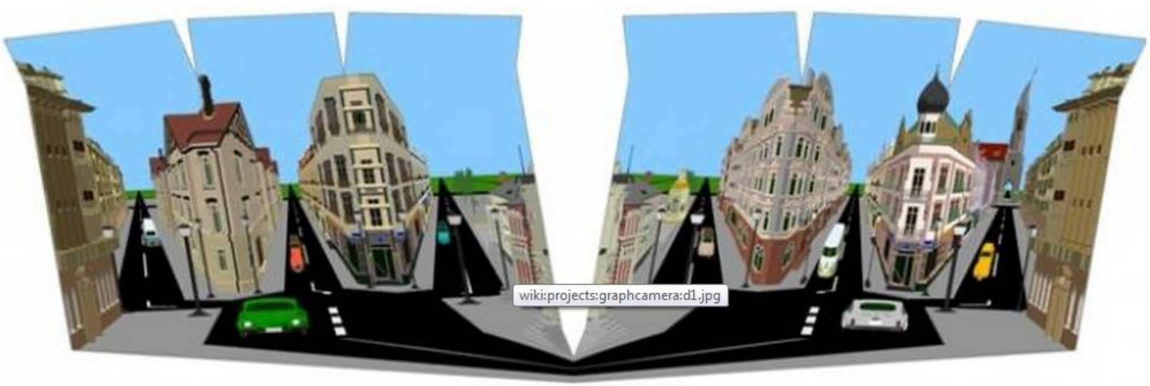

Enhanced street-level navigation

[Popescu-SIGA09]

Paraboloidal Catadioptric Camera

A paraboloidal catadioptric camera

Motorized cart with camera, computer, battery, radio remote control

Ideal Camera Model

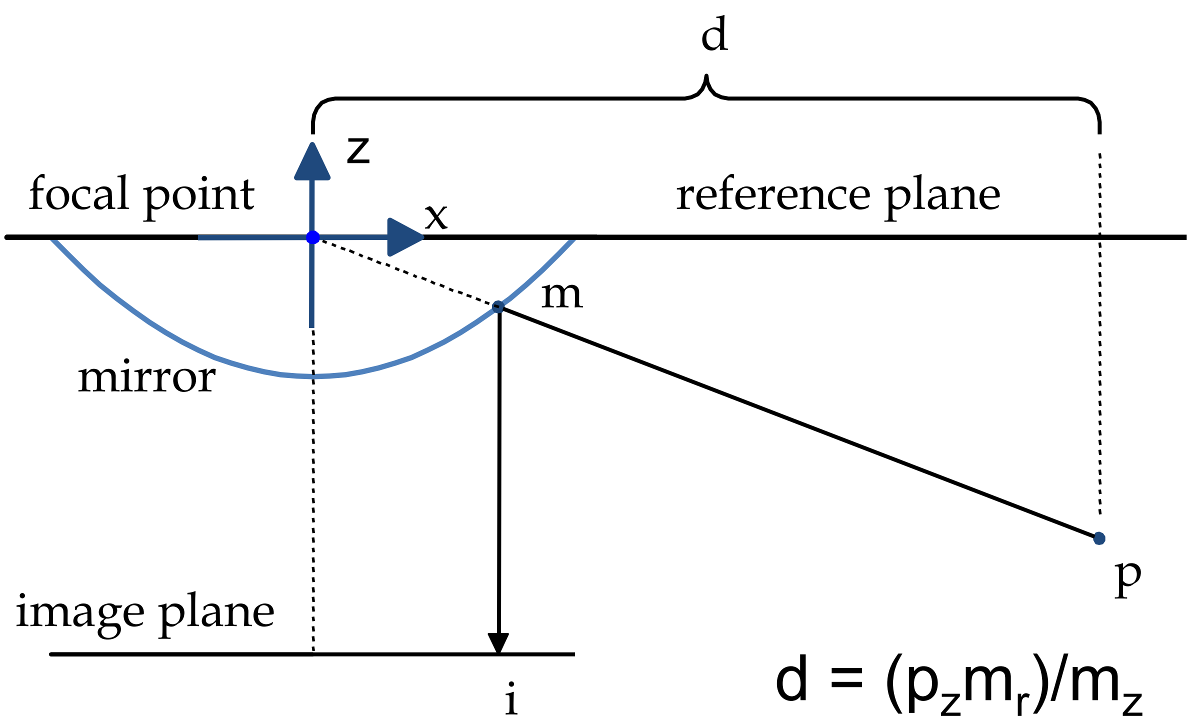

An ideal paraboloidal catadioptric setup for computing distance between the mirror's focal point and a 3D point

Our Camera Model

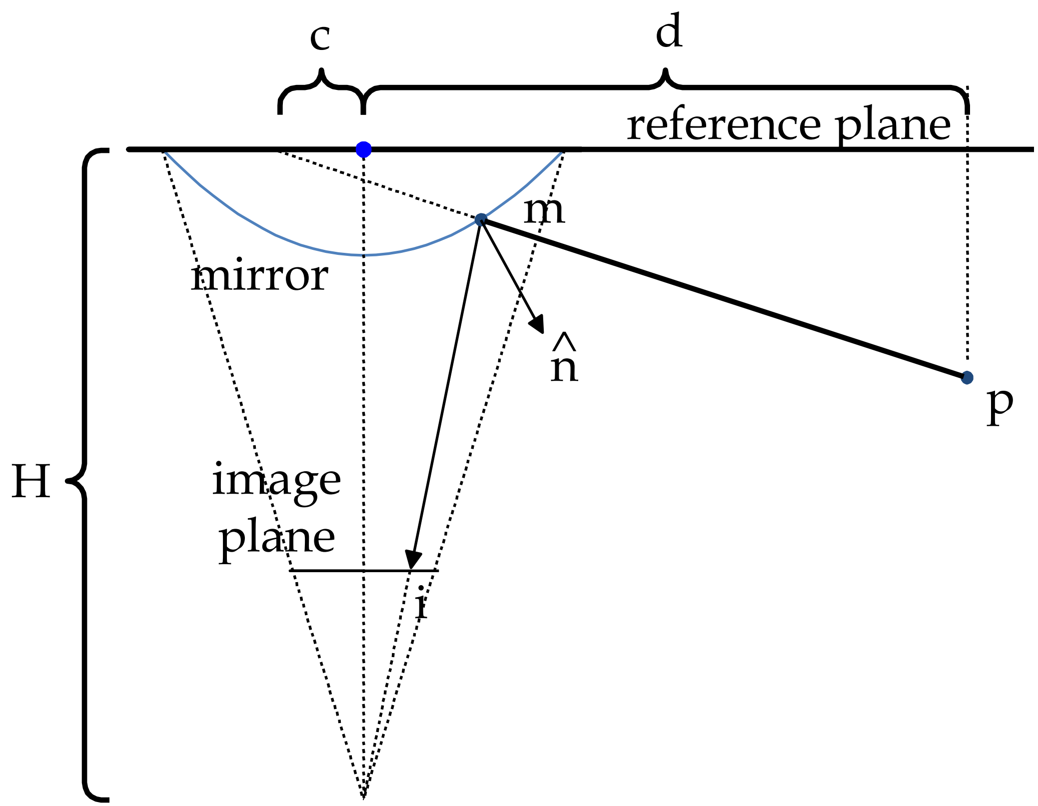

A paraboloidal catadioptric setup that accounts for perspective projection occurring in a practical system

Our Camera Model

- Assuming incident equals reflected angle:

$$\frac{i-m}{\|i-m\|}\cdot\frac{\hat{n}}{\|\hat{n}\|}=\frac{p-m}{\|p-m\|}\cdot\frac{\hat{n}}{\|\hat{n}\|}$$

- And given a 3D point *p*, mirror radius *r*, convergence distance *H*, we group and rewrite in terms of m_r:

$$m_r^5 - p_r m_r^4 + 2r^2 m_r^3 + (2p_r rH - 2r^2 p_r) m_r^2 + (r^4 - 4r^2 p_z H) m_r - (r^4 p_r + 2r^3 H p_r) = 0$$

- To obtain a new expression for distance *d*:

$$\mathbf{d = (p_z m_p)/m_z - m_z/\tan(\alpha) + m_r}$$

Pose Estimation Setup

Our pose estimation algorithm uses beacons placed in the environment to triangulate position and orientation of the camera moving in a plane.

Position and Orientation

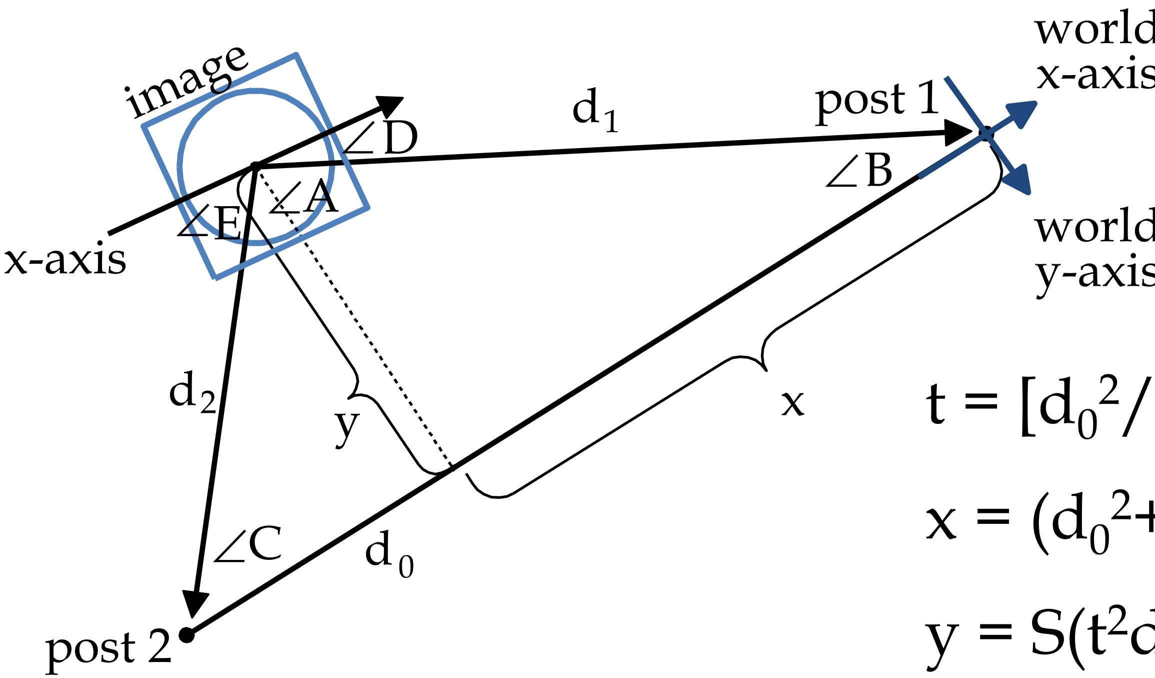

$$t = [d_0^2/(d_1^2+d_2^2-2d_1d_2\cos A)]^{1/2}$$

$$x = (d_0^2+t^2d_1^2-t^2d_2^2)/(2d0)$$

$$y = S(t^2d_1^2-x^2)^{1/2}$$

Our algorithm tracks the positions of small light bulbs and obtains camera position and orientation by solving an over-determined system.

Pose Estimation Error

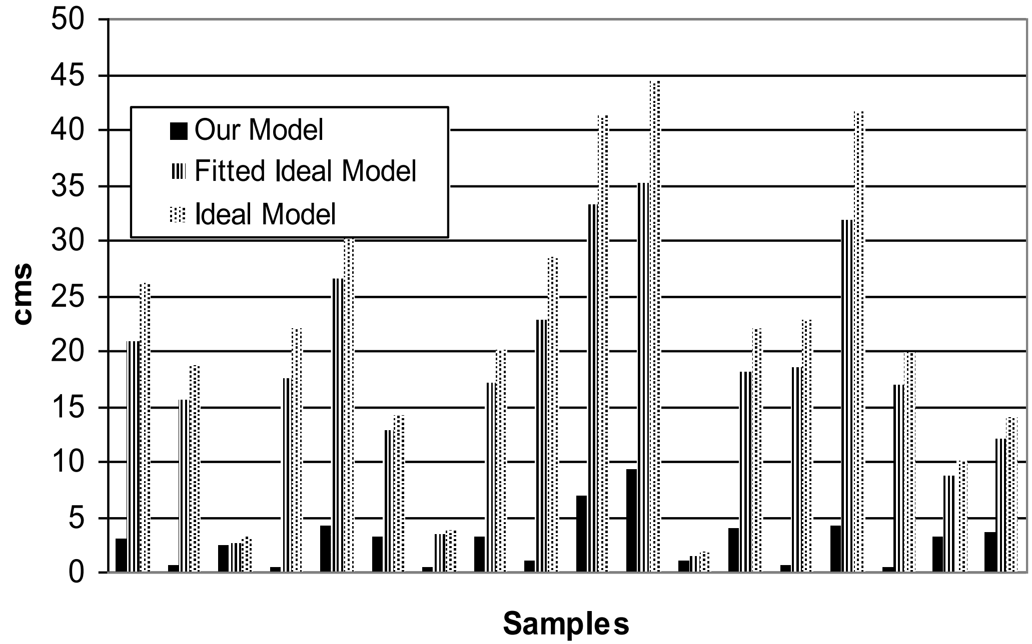

We achieve approximately an order of magnitude improvement over assuming an ideal catadioptric camera setup (as a percentage of the room diameter, mean error is 0.56% and σ=0.48%).

Satellite Linear Array Camera

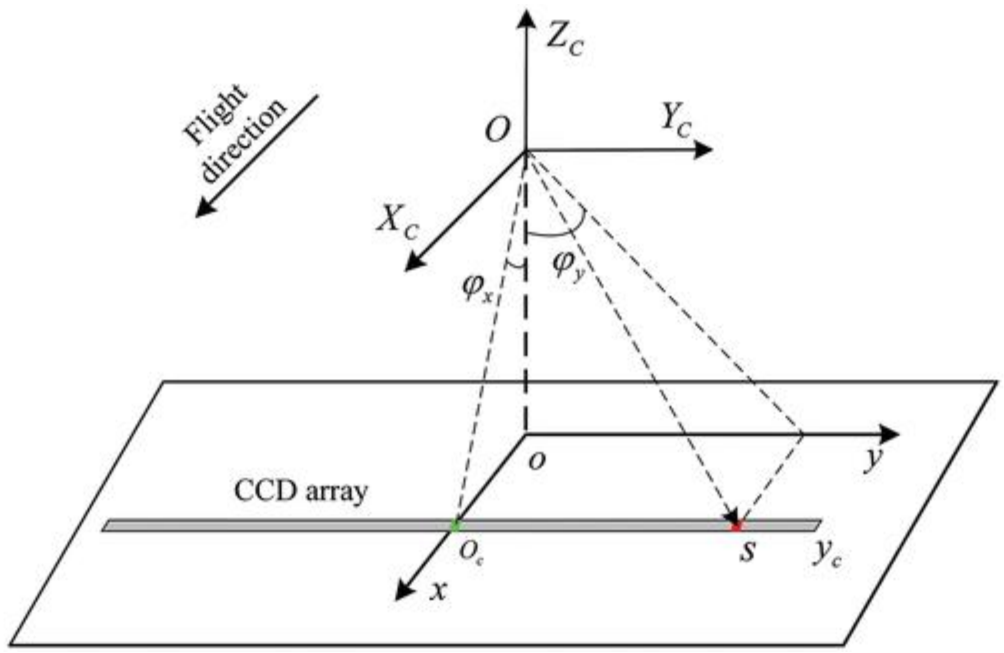

(Pushbroom camera)
A single line of thousands of electronic sensors (pixels) captures a thin strip of the Earth's surface at any given instant.

Satellite Linear Array Camera

- Rational Polynomial camera provides an abstraction:
- $u = \frac{N_U(x)}{D_u(x)}$ and $v = \frac{N_v(x)}{D_v(x)}$

Where x is the homogeneous coordinate of a 3D point, (u, v) is the corresponding image point, and N and D are polynomials of degree n.

Rational Polynomial Camera

- $u = N_u(x)/D_u(x)$ and $v = N_v(x)/D_v(x)$

- Consider case $n = 3$ and $(r = 4)$, then have 20 unknowns per N_u… so 80 total unknowns.
- (this is cubic RPC)
- And there are further specializations…

[Hartley and Saxena, 2001]

Rational Polynomial Camera

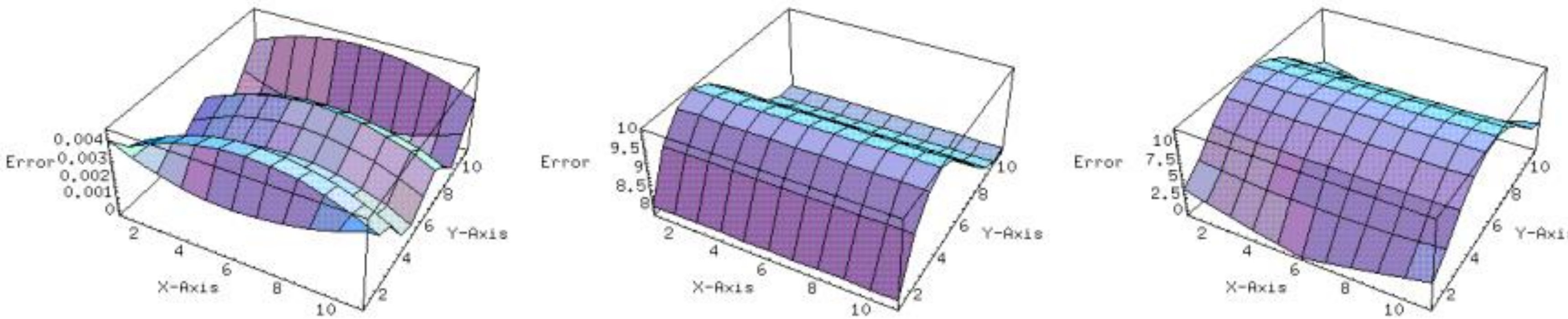

Cubic model — LP model — Perspective model

Figure 1: *Fitting error for synthetic SAR data using Cubic, Perspective and Linear Pushbroom models. The graphs show the error for points in the plane* $z = 0$, *but for fitting, data points at altitdues between -500m and 500m were used. The average error for Perspective and LP sensors was approximately 6 pixels, with a maximum of 10 pixels. The error achieved with the Cubic camera was only 0.02 pixels.*

General Linear Camera

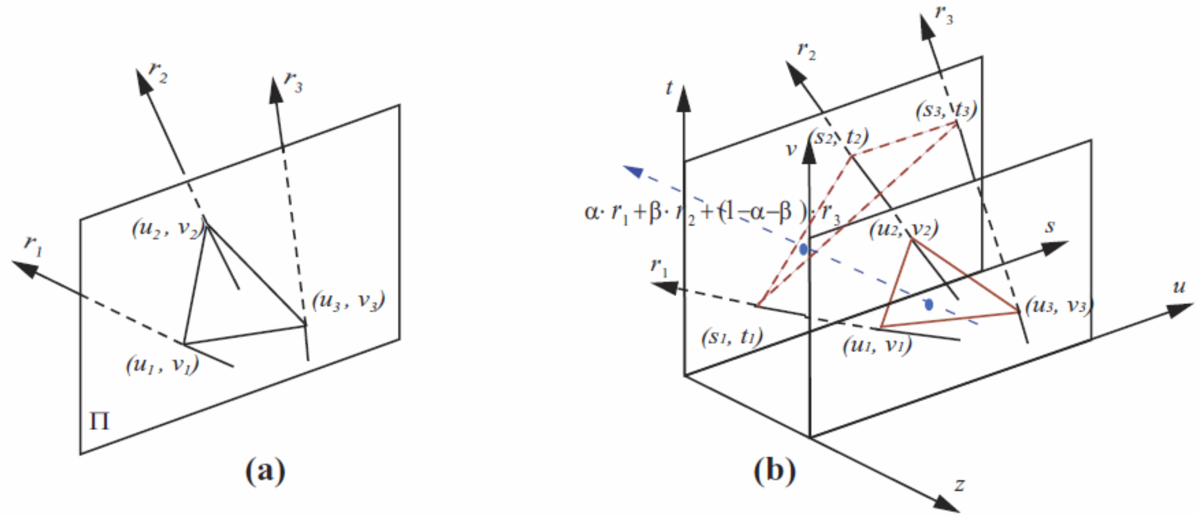

Fig. 1. General Linear Camera Model. a)A GLC is characterized by three rays originated from the image plane. b)It collects all possible affine combination of three rays.

[Yu-ECCV04]

General Linear Camera

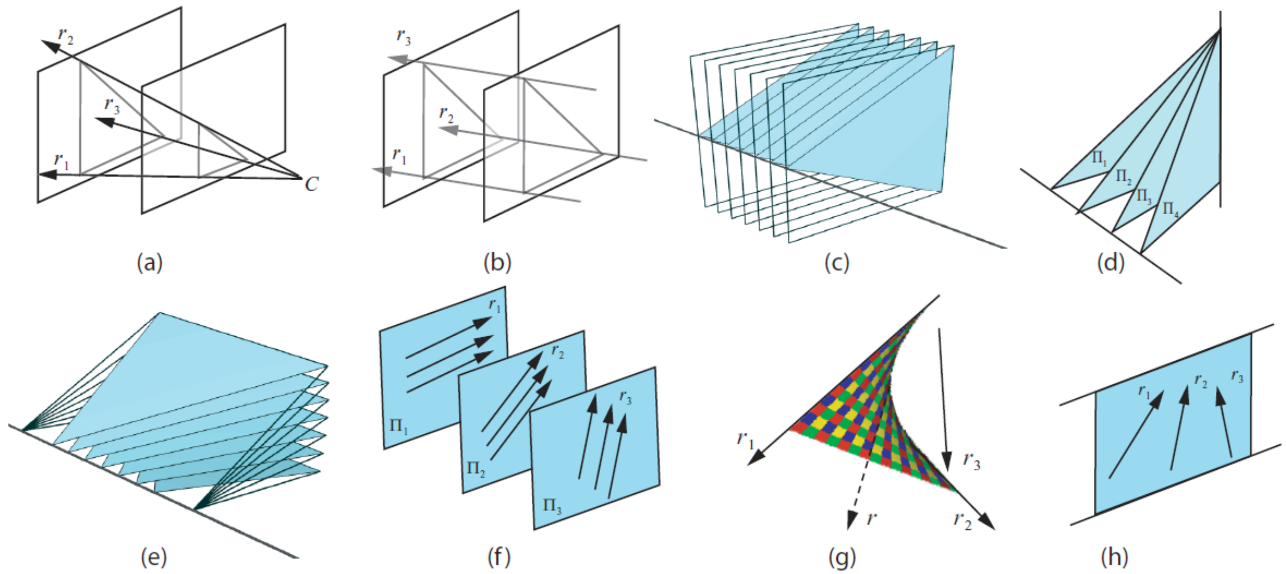

FIG. 1. *General Linear Camera Models. (a) In a pinhole camera, all rays pass through a single point. (b) In an orthographic camera, all rays are parallel. (c) In a pushbroom, all rays lie on a set of parallel planes and pass through a line. (d) In a cross slit camera, all rays pass through two non-coplanar lines. (e) In a pencil camera, all coplanar rays originate from a point on a line and lie on a specific plane through the line. (f) In a twisted orthographic camera, all rays lie on parallel twisted planes and no rays intersect. (g) In an bilinear camera, no two rays are coplanar and no two rays intersect. (h) In an EPI camera, all rays lie on a 2D plane.*

General Linear Camera

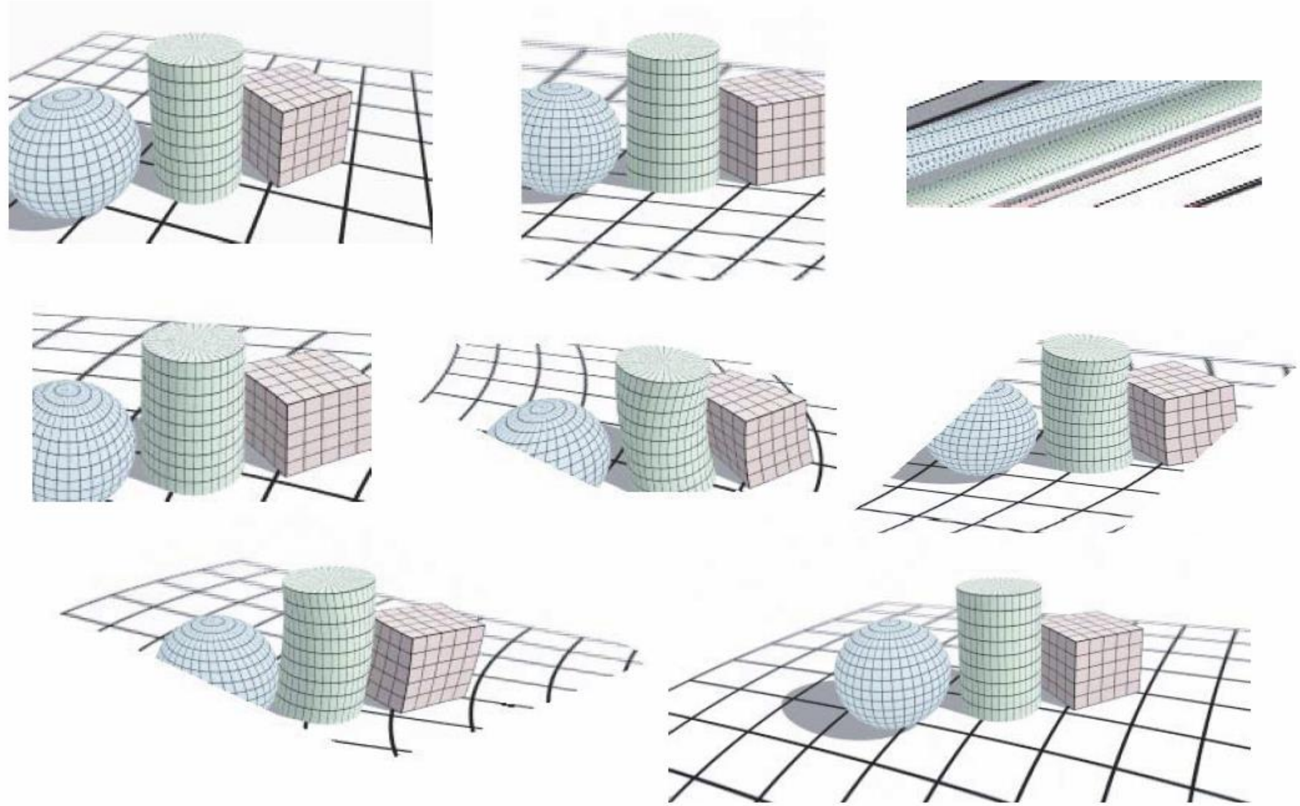

Fig. 5. Comparison between synthetic GLC images. From left to right, top row: a pinhole, an orthographic and an EPI; middle row: a pushbroom, a pencil and an twisted orthographic; bottom row: a bilinear and an XSlit.

General Linear Camera

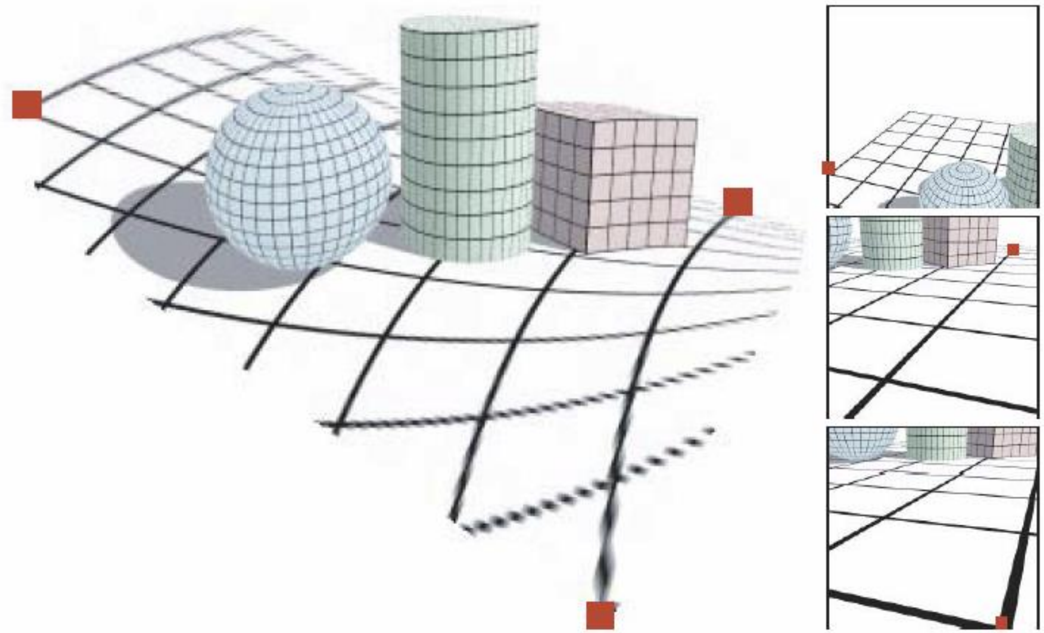

Fig. 7. A multiperspective bilinear GLC image synthesized from three pinhole cameras shown on the right. The generator rays are highlighted in red.

General Linear Camera

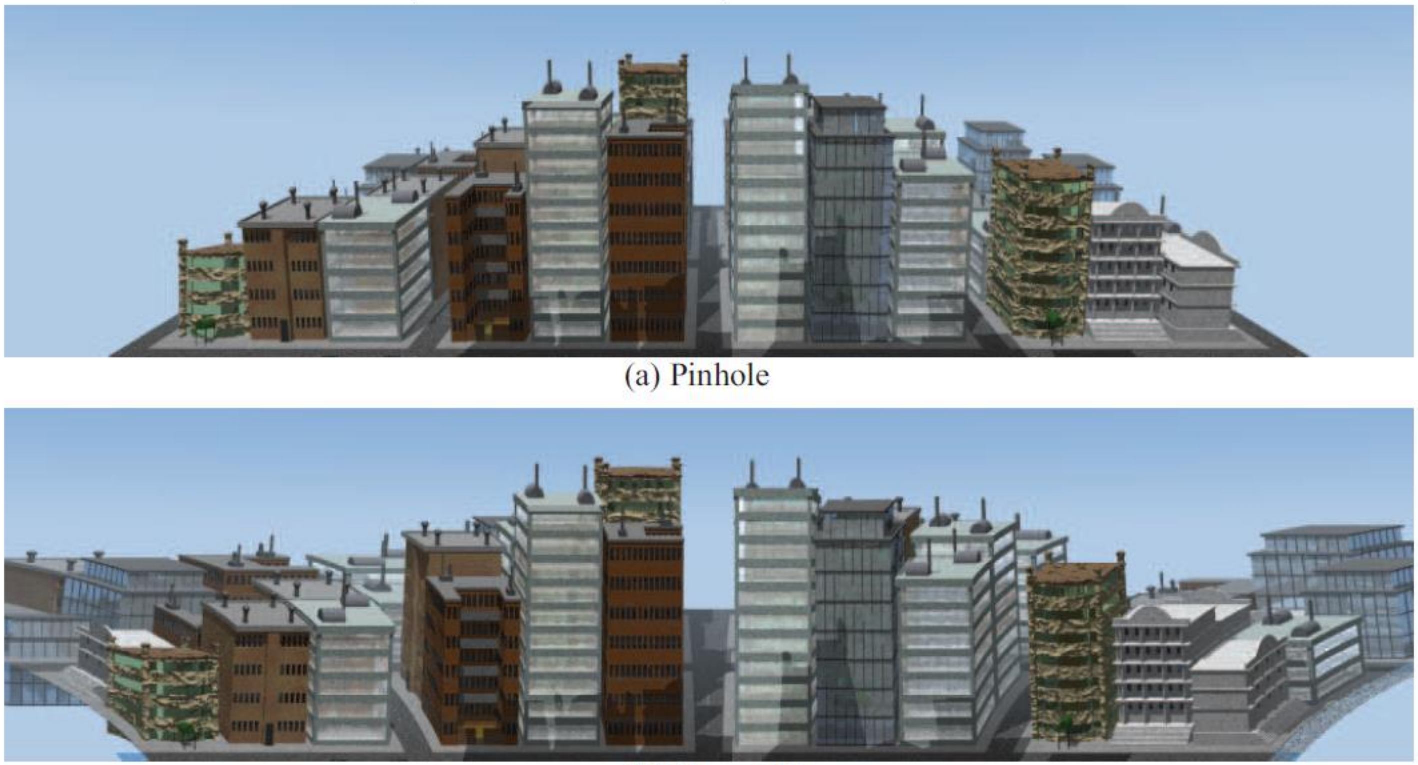

(a) Pinhole

(b) Cross-Slit

FIG. 11. *Panoramas of city scene rended using (a)pinhole camera and (b)cross-slit camera.*

GLC Papers

- Multiperspective Modeling and Rendering using General Linear Cameras
  - Yu, Ding, McMillan; Comm in Info Systems, 7(4), 2007
- General Linear Cameras
  - Yu, McMillan, ECCV, 2004